

Spin State of the Cobalt(II) Complex with *N,N'*-Disubstituted 2,6-Bis(pyrazol-3-yl)pyridine

E. A. Khakina^a, G. L. Denisov^a, I. A. Nikovskii^a, A. V. Polezhaev^{a, b}, and Yu. V. Nelyubina^{a, b, *}

^a Nesmeyanov Institute of Organoelement Compounds, Russian Academy of Sciences, Moscow, Russia

^b Bauman Moscow State Technical University, Moscow, Russia

*e-mail: unelya@ineos.ac.ru

Received November 12, 2021; revised November 29, 2021; accepted November 30, 2021

Abstract—The reaction of a new *N,N'*-disubstituted 2,6-bis(pyrazol-3-yl)pyridine ligand (L) with $\text{Co}(\text{ClO}_4)_2 \cdot 6\text{H}_2\text{O}$ gave cobalt(II) complex $[\text{Co}(\text{L})_2](\text{ClO}_4)_2$ (**I**), which was characterized by elemental analysis, mass spectrometry, NMR spectroscopy, and X-ray diffraction (CIF file CCDC no. 2121030). According to the Evans methods, NMR spectroscopy, and analysis of the temperature dependence of the NMR spectra, which are used to identify the spin state of paramagnetic compounds in solution, the cobalt(II) ion in complex **I** occurs in the high-spin state and does not undergo temperature-induced spin transition in the 235–345 K range.

Keywords: bis(pyrazol-3-yl)pyridine, Evans method, cobalt(II) complex, X-ray diffraction, spin state, NMR spectroscopy

DOI: 10.1134/S1070328422060021

INTRODUCTION

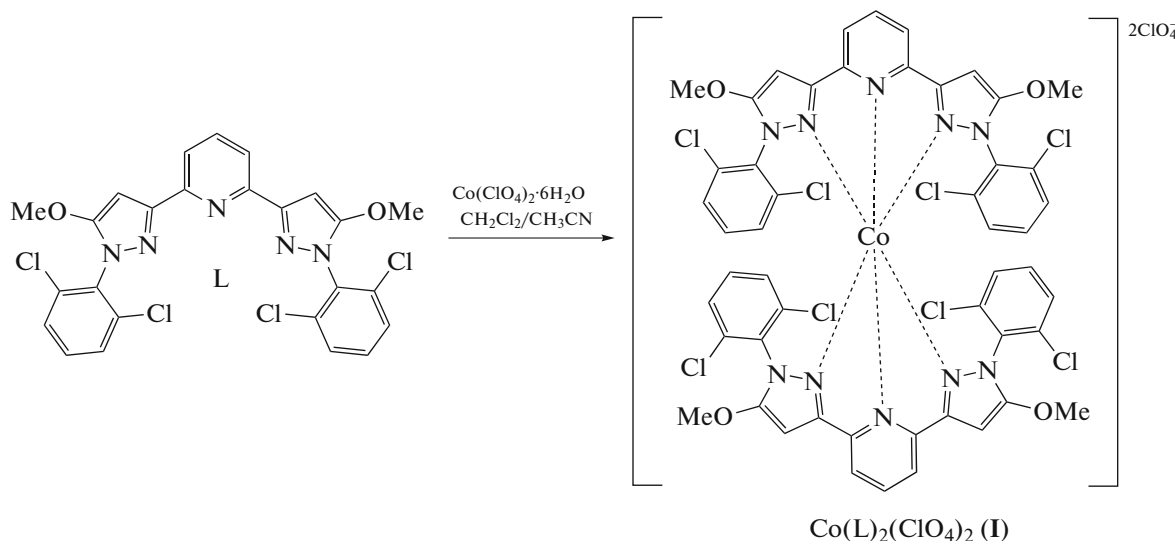
Some complexes of $3d^4$ – $3d^7$ transition metals [1] can exist in two spin states, low-spin (LS) and high-spin (HS) states, and switching between them occurs under the action of external impacts such as change in the temperature [2] and pressure [3], application of a magnetic field [4], or other physical stimuli [5]. The differences between the magnetic, dielectric, optical, and other properties [6] of these compounds in different spin states underlie their use to design ultradense data storage systems [7, 8], molecular switches, and other devices [4]. Most often, the ability to switch between the LS and HS states (so-called spin transition) is inherent in iron(II) and cobalt(II) complexes in the (pseudo)octahedral environment of nitrogen-containing heterocyclic ligands [1]. 2,6-Di(pyrazol-1-yl)pyridines are among the most studied classes of such ligands [9], which is due to the ease of their chemical modification and synthetic accessibility [10]. For example, these features made it possible to reveal a clear relationship between the nature of substituents in various positions of 2,6-di(pyrazol-1-yl)pyridine and spin transition temperature in the iron(II) complexes [11].

The lack of a similar dependence for isomeric 2,6-di(pyrazol-3-yl)pyridine ligands is due to the presence of NH groups, capable of hydrogen bonding to solvent molecules and/or counter-ions, in position 1 of the

pyrazolyl ring [12]. The formation of these hydrogen bonds near metal-coordinated nitrogen atoms has an unpredictable effect on the spin state of the metal [13]. However, until recently, all attempts to introduce substituents into this position of 2,6-di(pyrazol-3-yl)pyridines resulted in metal complexes exclusively in the HS state [13]; this precluded the molecular design of compounds with spin transitions using this class of N-heterocyclic ligands by analogy with isomeric 2,6-di(pyrazol-1-yl)pyridines.

Recently, we proposed such a design of N-substituent, namely, *ortho*-substituted aryl group, which does not prevent the spin transition in iron(II) [14] and cobalt(II) complexes [15] and, moreover, allows one to control the spin transition temperature by introducing substituents into other positions of the 2,6-di(pyrazol-3-yl)pyridine ligand [16, 17].

In this study, we synthesized a new representative of this series of *N,N'*-disubstituted ligands, 2,6-bis(1-(2,6-dichlorophenyl)-5-methoxy-1*H*-pyrazol-3-yl)pyridine (L), and the cobalt(II) complex $[\text{Co}(\text{L})_2](\text{ClO}_4)_2$ (**I**) of this ligand (Scheme 1). The spin state of the complex was studied by X-ray diffraction and NMR spectroscopy, which is traditionally used to search for new compounds with a temperature-induced spin transition [13].



Scheme 1.

EXPERIMENTAL

All operations related to the synthesis of ligand L and its complex were carried out in air using commercially available organic solvents, which were distilled under argon. Cobalt perchlorate hexahydrate $\text{Co}(\text{ClO}_4)_2 \cdot 6\text{H}_2\text{O}$ (Sigma-Aldrich) was used as received. 3,3'-(Pyridine-2,6-diyl)bis(1-(2,6-dichlorophenyl)-1H-pyrazol-5-ol), which served as a precursor for the synthesis of ligand L, was prepared by a known procedure [14]. Analysis for carbon, nitrogen, and hydrogen was performed on a Carlo Erba 1106 microanalyzer.

Synthesis of 2,6-bis(1-(2,6-dichlorophenyl)-5-methoxy-1H-pyrazol-3-yl)pyridine (L). 3,3'-(Pyridine-2,6-diyl)bis(1-(2,6-dichlorophenyl)-1H-pyrazol-5-ol) (0.5 g, 0.937 mmol) was dissolved in DMF (20 mL) in a 50-mL flask. Cesium carbonate (0.763 g, 2.343 mmol) and Me_2SO_4 (186 μL , 1.969 mmol) were added to the solution. The resulting suspension was stirred at 70°C for 8 h. Then the reaction mixture was cooled to room temperature and poured into distilled water (70 mL). The precipitate thus formed was collected on a filter, washed with water, and dried in a high vacuum. The product was used without further purification. The yield was 448 mg (85%).

For $\text{C}_{25}\text{H}_{17}\text{N}_5\text{O}_2\text{Cl}_4$

Anal. calcd., %	C, 53.50	H, 3.05	N, 12.48
Found, %	C, 53.55	H, 3.09	N, 12.53

^1H NMR (DMSO- d_6 ; 400 MHz; δ , ppm): 3.97 (s, 6H, OMe), 6.59 (s, 2H, Pz-CH), 7.59 (t, 2H, $3J_{\text{HH}} = 8.0$ Hz, *p*-Ph), 7.70 (d, 4H, $3J_{\text{HH}} = 8.0$ Hz, *m*-Ph), 7.83 (s, 3H, *p*-Py + *m*-Py). ^{13}C NMR (DMSO- d_6 ; 101 MHz; δ , ppm): 59.97 (s, Me), 84.13 (s, 4-Pz),

118.80 (s, 3-Py), 129.49 (s, 4-Ph), 132.74 (s, 3-Ph), 133.25 (s, 2-Ph), 134.74 (s, 1-Ph), 137.89 (s, 4-Py), 151.47 (s, 3-Pz), 152.40 (s, 5-Pz), 157.32 (s, 2-Py). HR-MS (ESI $^+$). m/z : $[\text{C}_{25}\text{H}_{17}\text{Cl}_4\text{N}_5\text{O}_2]^+$, calcd.: 582.0029; found: 582.0014.

Synthesis $[\text{Co}(\text{L})_2](\text{ClO}_4)_2$ (I). A solution of $\text{Co}(\text{ClO}_4)_2 \cdot 6\text{H}_2\text{O}$ (0.0037 g, 0.01 mmol) in acetonitrile (0.1 mL) was added to a solution of ligand L (0.0112 g, 0.02 mmol) in a mixture of dichloromethane (0.3 mL) and acetonitrile (0.1 mL). The resulting mixture was stirred at room temperature for 1 h, and then dichloromethane was distilled off on a rotatory evaporator. The residue after evaporation was kept for 12 h at -18°C . The resulting crystalline precipitate was separated from the liquid phase by decantation and dried in air. The yield was 11 mg (80%).

MS (ESI), m/z : $[\text{Co}(\text{L})_2]^{2+}$, calcd. 590.5, found. 590.8; $[\text{Co}(\text{L})_2](\text{ClO}_4)_2^+$, calcd. 1279.9, found. 1279.9. ^1H NMR (acetonitrile- d_3 ; 300 MHz; 292 K; δ , ppm): -3.02 (br.s., 2H, *p*-Py), 1.47 (br.s., 8H, *m*-Ph), 2.06 (br.s., 4H, *p*-Ph), 13.88 (br.s., 12H, Me), 19.21 (br.s., 4H, Pz), 56.66 (br.s., 4H, *m*-Py).

X-ray diffraction study of the single-crystals of complex I, obtained by slow evaporation of the solvent (an acetonitrile and dichloromethane mixture in 2 : 1 ratio (v/v)) in air, was carried out on a Bruker APEX2 DUO CCD diffractometer (MoK_α radiation, graphite monochromator, ω -scan mode). The structure was solved using the ShelXT software [18] and refined in the full-matrix least-squares method in the anisotropic approximation on F_{hkl}^2 using the Olex2 program [19]. The positions of hydrogen atoms were calculated geometrically and refined in the isotropic approximation by the riding model. The disordered solvent (acetonitrile) molecules were described as a diffuse contri-

Table 1. Crystallographic data, X-ray experiment details, and structure refinement parameters for complex **I**

Parameter	Value
Molecular formula	C ₅₀ H ₃₄ N ₁₀ O ₁₂ Cl ₁₀ Co
<i>M</i>	1380.30
<i>T</i> , K	120
System	Monoclinic
Space group	<i>P</i> 2 ₁ / <i>c</i>
<i>Z</i>	4
<i>a</i> , Å	22.2478(14)
<i>b</i> , Å	24.8150(16)
<i>c</i> , Å	22.6356(16)
α, deg	90
β, deg	149.147(2)
γ, deg	90
<i>V</i> , Å ³	6409(8)
ρ(calcd.), g cm ⁻³	1.431
μ, cm ⁻¹	7.47
<i>F</i> (000)	2788
2θ _{max} , deg	56
Number of measured reflections	73821
Number of unique reflections	15457
Number of reflections with <i>I</i> > 3σ(<i>I</i>)	11423
Number of refined parameters	772
<i>R</i> ₁	0.0598
<i>wR</i> ₂	0.1836
GOOF	1.036
Residual electron density (max/min), e Å ⁻³	1.336/-1.664

bution to the total scattering using the Solvent Mask option of the Olex2 program [19]. The main crystallographic data for **I** are summarized in Table 1.

The atom coordinates and other structural parameters of **I** were deposited with the Cambridge Crystallographic Data Centre (CCDC no. 2121030; <http://www.ccdc.cam.ac.uk/>).

The mass spectrometric analysis of complex **I** was performed using an LCMS-2020 electrospray ionization liquid chromatograph/mass spectrometer (Shimadzu, Japan) with a quadrupole detector (positive and negative ion modes, *m/z* in the 50–2000 range). The desolvation line and heating block temperatures were 250 and 400°C, respectively. Nitrogen (99.5%) was used as the spray and drying gas, and acetonitrile (99.9+%, Chem-Lab) with a 0.4 mL/min flow rate was used as the mobile phase. The sample volume was 3 μL (concentration of 0.2 mg/mL; acetonitrile as the solvent).

¹H and ¹³C NMR spectra were recorded in acetonitrile-d₃ and DMSO-d₆ on Bruker Avance 300 and 400 spectrometers operating at 300.15 and 400 MHz for protons, respectively. The chemical shifts (δ, ppm) in the spectra were referred to the residual solvent signal (1.94 ppm for ¹H in acetonitrile-d₃; 2.5 ppm for ¹H and 39.52 ppm for ¹³C in DMSO-d₆) or to the signal of 1% Me₄Si impurity (0.0 ppm for ¹H). The ¹H NMR spectra of **I** were recorded using the following parameters: 250 ppm spectral range, 0.2 s recording time, 0.6 s relaxation delay, 9.5 μs pulse duration, and 64 acquisitions. The obtained free induction decays for increasing the signal-to-noise ratio were processed using exponential weighting with a factor of up to 3.

The temperature dependence of the magnetic susceptibility of complex **I** in acetonitrile-d₃ was estimated by the Evans method [20] in the temperature range of 235–345 K using an NMR tube with a coaxial insert. The inner (control) tube was filled with aceto-

Table 2. Selected geometric parameters for complex **I** according to X-ray diffraction data at 120 K*

Parameter	I
Co—N(Py), Å	2.025(3)/2.030(3)
Co—N(Pz), Å	2.107(3)–2.131(3)
θ, deg	89.39(3)
N(Py)CoN(Py), deg	178.56(11)
S(TP-6)	11.244
S(OC-6)	3.325

* θ is the dihedral angle between the root-mean-square planes of the 2,6-bis(pyrazol-3-yl)pyridine ligands, N(Py) and N(Pz) correspond to the nitrogen atoms of the pyridine and pyrazol-3-yl moieties. S(TP-6) and S(OC-6) are deviations of the shape of CoN_6 polyhedron from the ideal trigonal prism (TP-6) and ideal octahedron (OC-6), respectively.

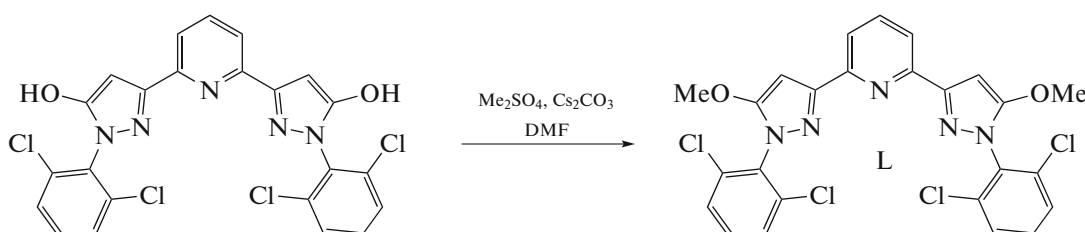
nitrile-d₃ with addition of 1% Me_4Si , while the outer tube contained a solution of a paramagnetic complex (5.1 mg/cm³) in acetonitrile-d₃ with the same Me_4Si concentration. The molar magnetic susceptibility was calculated from the difference between the Me_4Si chemical shifts in pure acetonitrile-d₃ and in the acetonitrile-d₃ solution of the complex ($\Delta\delta$ in Hz) using the following equation:

$$\chi_M = \frac{\Delta\delta M}{v_0 S_f c} - \chi_M^{\text{dia}},$$

where M is the molecular weight of the complex, g/mol; v_0 is the spectrometer frequency, Hz; S_f is the shape factor of the magnet ($4\pi/3$); c is the concentration of the complex, g/cm³; χ_M^{dia} is the molar diamagnetic contribution to the paramagnetic susceptibility calculated using the Pascal constants [21]. The concentration c was calculated for each temperature according to the change in the solvent density ρ : $c_T = m_s\rho/m_{\text{sol}}$, where $m_s\rho$ is the mass of the complex, m_{sol} is the mass of the solution.

RESULTS AND DISCUSSION

2,6-Bis(1-(2,6-dichlorophenyl)-5-methoxy-1*H*-pyrazol-3-yl)pyridine (**L**) was synthesized (Scheme 1) from 3,3'-(pyridine-2,6-diyl)bis(1-(2,6-dichlorophenyl)-1*H*-pyrazol-5-ol) prepared by a reported procedure [14], which was methylated with dimethyl sulfate in the presence of cesium carbonate (Scheme 2).

**Scheme 2.**

Due to poor solubility of ligand **L** in pure acetonitrile, the subsequent reaction with cobalt(II) perchlorate hexahydrate was carried out in a 3 : 2 (v/v) mixture of dichloromethane and acetonitrile. The reaction gave the homoleptic complex $[\text{Co}(\text{L})_2](\text{ClO}_4)_2$ (**I**) (Scheme 1), which was characterized by mass spectrometry (Fig. 1), NMR spectroscopy (Fig. 2), and single crystal X-ray diffraction (Fig. 3). The last-mentioned method made it possible to determine the spin state of the cobalt(II) ion, which proved to be in the high-spin state at a temperature of 120 K. The Co—N distances to the nitrogen atoms of two bis(pyrazol-3-yl)pyridine ligands (C.N. 6) (Table 2) were characteristic of cobalt(II) complexes in the HS state (2.0–2.2 Å [1]).

According to X-ray diffraction data, the coordination environment of the cobalt(II) ion in complex **I** was close to octahedral (Fig. 4). The θ angle between the root-mean-square planes of the two ligands and the N(Py)CoN(Py) angle, which amount to 90° and 180° in the case of ideal octahedron, were 89.39(3)° and 178.56(11)°, respectively. The shape of the CoN_6 coordination polyhedron was characterized more accurately by “shape measures” [22], which describe its deviation from the ideal octahedron (OC-6). The lower this value, the closer the geometry to an ideal polyhedron. In complex **I**, the octahedral shape measure S(OC-6), estimated from X-ray diffraction data using the Shape 2.1 software program [22], was 3.325 (Table 2). For comparison, the shape measure characterizing the deviation from one more ideal six-vertex

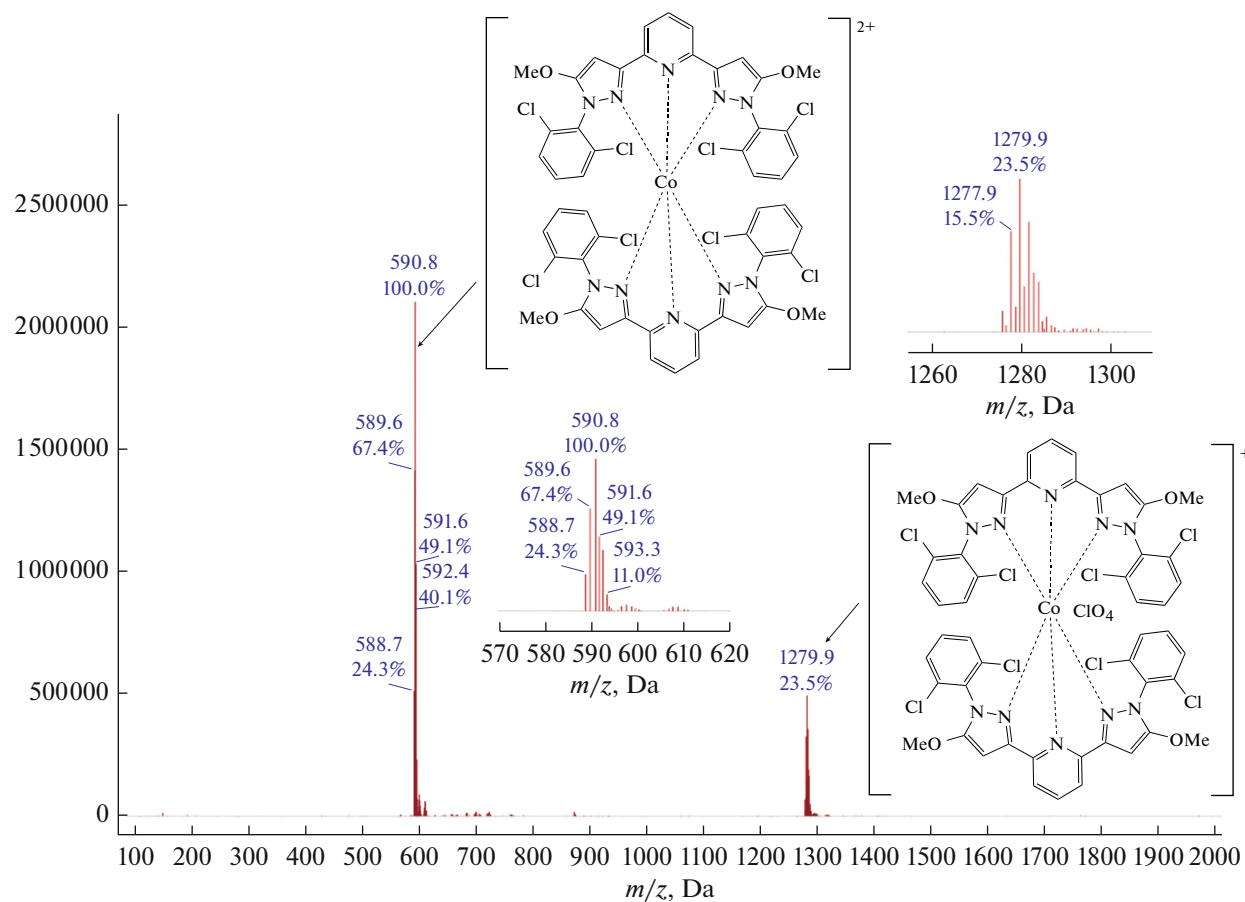


Fig. 1. Electrospray ionization (ESI) mass spectrum of complex **I** (positive ion mode).

polyhedron, trigonal prism (TP-6), which is traditionally encountered in HS iron(II) complexes with *N*-heterocyclic ligands [23], was much higher: 11.244 (Table 2).

The minor deviation of the shape of cobalt(II) coordination polyhedron in complex **I** from ideal octahedron is, first of all, due to the rigidity of the bis(pyrazol-3-yl)pyridine ligand [24]. Similar “shape measures” were previously found for HS cobalt(II) complexes with other bis(pyrazol-3-yl)pyridines [25, 26]. The formation of this rigid structure is facilitated by the intramolecular stacking interactions between the aromatic pyridine moieties and *N*-aryl substituents, with the angle between them being 2.68(13)°–5.17(12)° and the distance between their centroids being 3.641(2)–3.725(2) Å. In addition, chlorine atoms in the *ortho*-positions of these substituents participate in pairs in the formation of intramolecular halogen bonds (Cl...Cl, 3.1912(17)–3.2865(15) Å; CClCl, 133.18(14)°–140.47(13)°) [27].

The chlorine atoms Cl(2A) and Cl(4A) also form an intermolecular halogen bond (Cl...Cl, 3.3460(13) Å; CClCl, 153.27(13)°), which combines [Co(L)₂]²⁺ cations into infinite chains along the diagonal of the *ac* crys-

tallographic plane (Fig. 5). These chains are connected into a dense three-dimensional framework by weaker interactions, including Cl(1)...Cl(1A) and Cl(4)...Cl(3A) halogen bonds (Cl...Cl, 3.5236(14), 4.756(2) Å; CClCl, 159.71(12)°, 168.51(14)°), C–H...Cl contacts (C...Cl, 3.676(4) Å; CHCl, 145.0(2)°) between the neighboring [Co(L)₂]²⁺ cations, and C–H...O contacts with the surrounding perchlorate anions (C...O, 3.189(10)–3.432(3) Å; CHO, 133.4(3)°–165.2(3)°).

Thus, the cobalt(II) ion in complex **I** in the crystal at 120 K occurs in the HS state, as unambiguously follows from its X-ray diffraction data at this temperature. Since crystal packing effects as the above-described intermolecular interactions can, in some cases, lead to the absence of spin transition [23, 28], the spin state of this complex was studied in solution using the Evans method of NMR spectroscopy traditionally used for this purpose [13]. In this experiment, a special coaxial insert containing a solution of a standard compound, e.g., TMS, is inserted into an NMR tube containing a solution of the paramagnetic complex and TMS of a known concentration in the same solvent. The difference between the TMS chemical shifts in the NMR spectrum recorded simultaneously

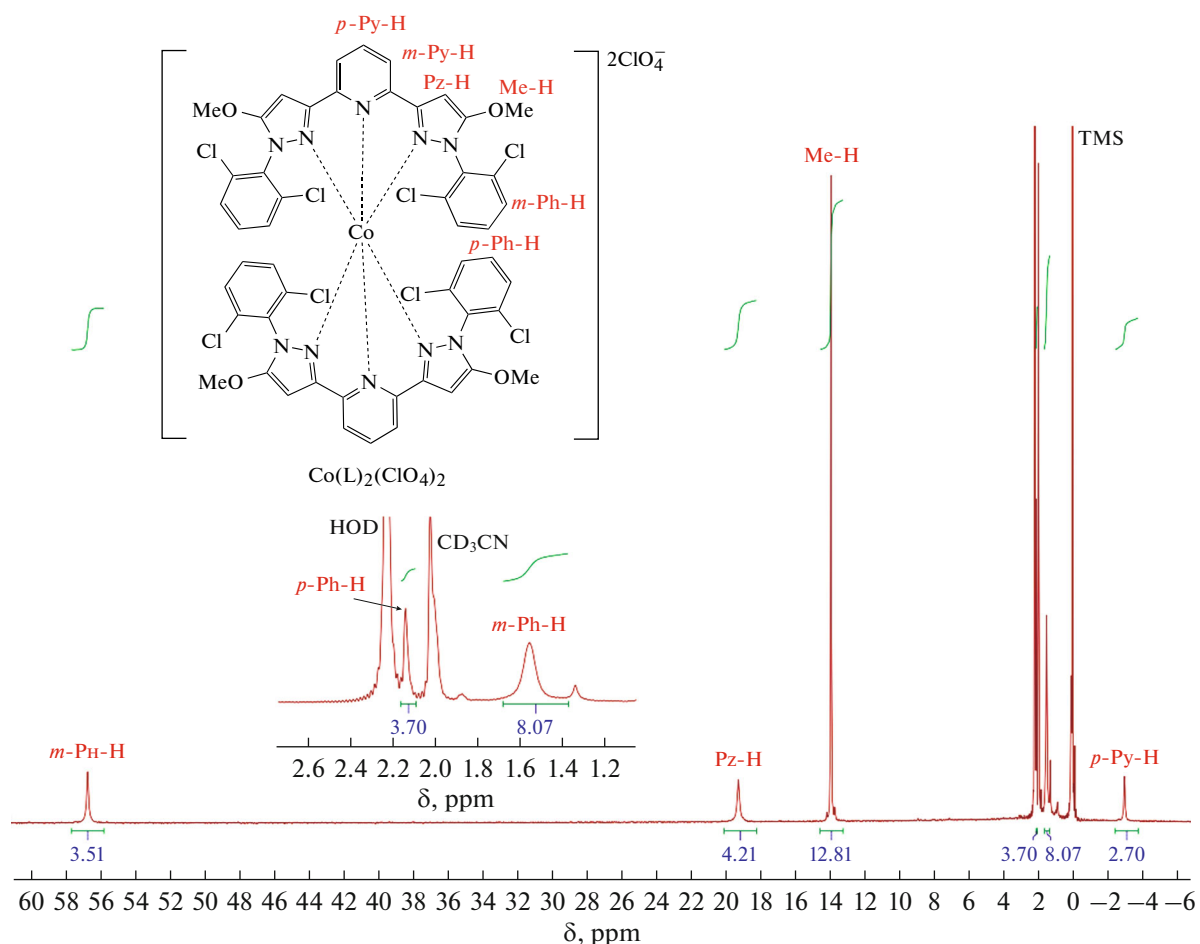


Fig. 2. ^1H NMR spectrum of complex I in acetonitrile- d_3 solution at room temperature.

for these two solutions can be used to calculate the magnetic susceptibility of the solution of the studied paramagnetic compound. Thus, it is possible to reliably determine the spin state of the metal ion and its possible change with temperature by recording the spectra at different temperatures.

The χT value of complex I in acetonitrile- d_3 calculated in this way (Fig. 6) deviates only insignificantly from the value of $2.7 \text{ cm}^3 \text{ mol}^{-1} \text{ K}$, corresponding to the cobalt(II) ion in the HS state ($S = 3/2$) over the whole temperature range of 235–345 K accessible for the given solvent.

The data on the HS state of the cobalt(II) ion in complex I obtained by the Evans method are additionally confirmed by the linear dependence of the chemical shifts of proton signals of the complex in the ^1H NMR spectra (recorded at different temperatures) on the reciprocal temperature (Fig. 7, 8). The observed chemical shifts δ_{H} in the ^1H NMR spectra of compounds that can exist in two spin states is the weighted average of the chemical shifts of the same nuclei for pure LS and HS states (η_{LS} and η_{HS} are the state populations):

$$\delta_{\text{H}} = \eta_{\text{LS}}\delta_{\text{LS}} + \eta_{\text{HS}}\delta_{\text{HS}}.$$

For the cobalt(II) complex in the paramagnetic LS state, the observed chemical shift (δ_{H}) of each nucleus can be represented as the sum of diamagnetic (δ_{dia}) and paramagnetic (δ_{par}) contributions [15]:

$$\begin{aligned} \delta_{\text{H}} &= \eta_{\text{LS}}(\delta_{\text{dia}}^{\text{LS}} + \delta_{\text{par}}^{\text{LS}}) + \eta_{\text{HS}}(\delta_{\text{dia}}^{\text{HS}} + \delta_{\text{par}}^{\text{HS}}) \\ &\approx \delta_{\text{dia}} + \eta_{\text{LS}}\delta_{\text{par}}^{\text{LS}} + \delta_{\text{par}}^{\text{HS}}(1 - \eta_{\text{HS}}) = \delta_{\text{dia}} + \delta_{\text{par}}. \end{aligned}$$

The diamagnetic contribution δ_{dia} , which is the same for the LS and HS states, is approximately equal to the chemical shift of the corresponding nucleus in the free ligand.

In the case of paramagnetic metal complexes that do not undergo the temperature-induced spin transition, the paramagnetic chemical shift depends linearly on the reciprocal temperature (Curie's law): $\delta_{\text{par}}^{\text{HS}} = A + BT^{-1}$. Conversely, the spin transition results in considerable deviations of chemical shifts of some nuclear from linear dependence [15]. It can be seen from our results that such deviations are not observed in the case of complex I, which confirms that

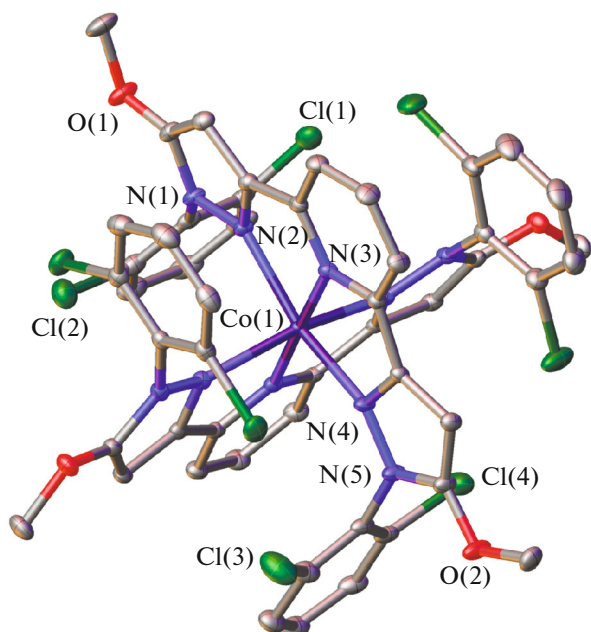


Fig. 3. General view of complex **I**. Here and below, the perchlorate anions and hydrogen atoms are not shown, the other atoms are presented as thermal ellipsoids ($\rho = 30\%$). The atom numbering is given only for the metal ion and selected heteroatoms.

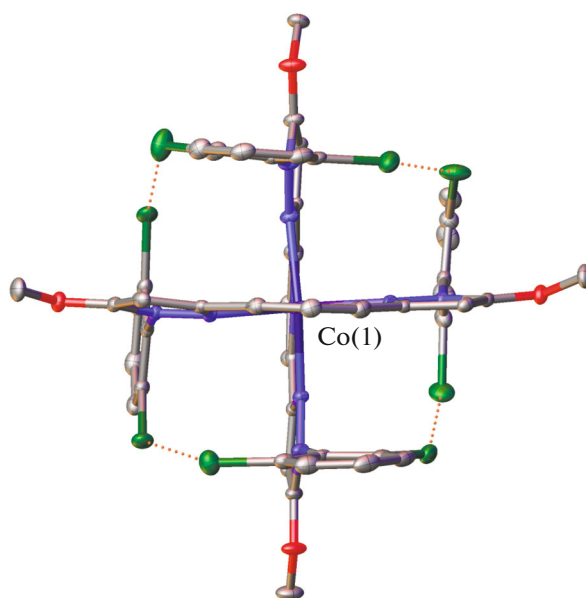


Fig. 4. Projection of complex **I** in the perpendicular direction illustrating the nearly octahedral shape of the cobalt(II) coordination polyhedron. The dotted lines show intramolecular halogen bonds.

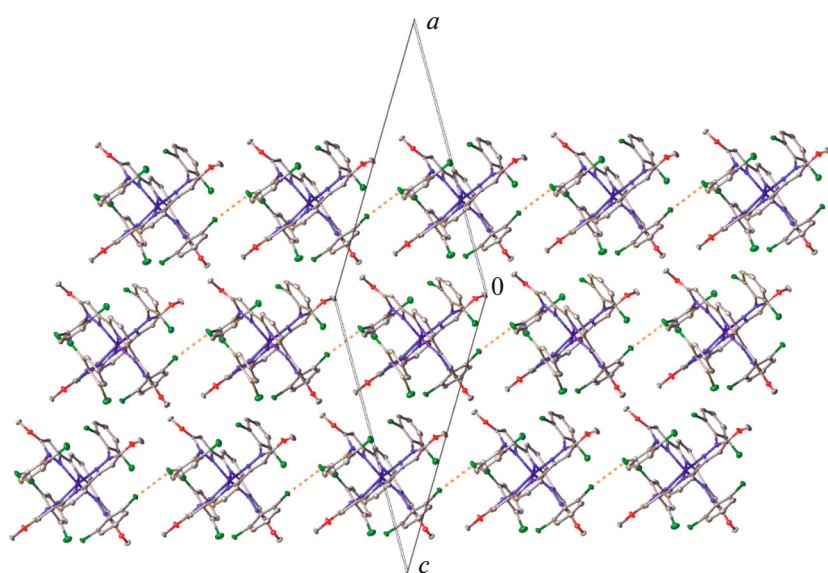


Fig. 5. Fragment of the crystal packing of complex **I** illustrating the formation of infinite chains in the crystal via halogen bonds (indicated by dotted lines).

no spin transition takes place in this complex over the whole temperature range.

Thus, we synthesized and characterized a new cobalt(II) complex with *N,N'*-disubstituted 2,6-bis(pyrazol-3-yl)pyridine. According to the results of

low-temperature X-ray diffraction study carried out for the complex (first of all, Co—N bond lengths), the cobalt(II) ion in this complex occurs in the HS state even at 120 K. It also does not undergo a temperature-induced spin transition in an acetonitrile solution in

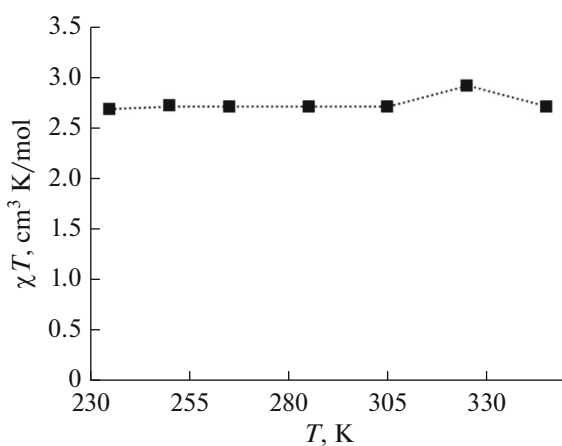


Fig. 6. Temperature dependence of the magnetic susceptibility of complex I in acetonitrile-d₃ according to NMR spectroscopy data (Evans method).

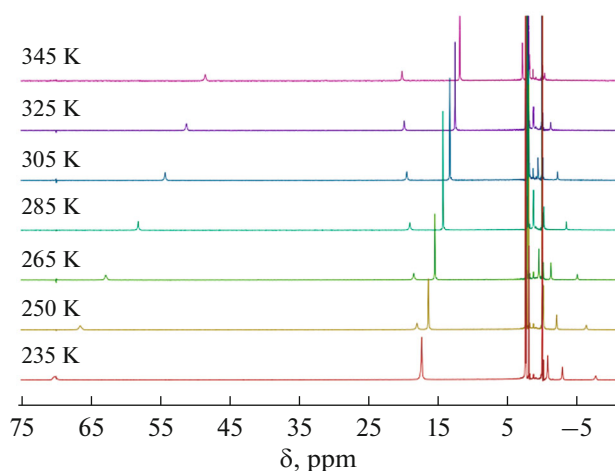


Fig. 7. ¹H NMR spectra measured at different temperatures for complex I in acetonitrile-d₃.

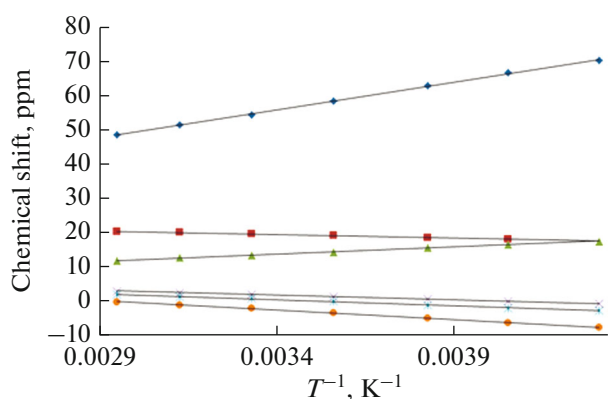


Fig. 8. ¹H NMR chemical shifts of complex I versus reciprocal temperature.

the temperature range of 235–345 K, which is confirmed by the data of the Evans method traditionally used for this purpose [13] and analysis of the temperature dependence of NMR chemical shifts [15]. However, presumably, the replacement of cobalt(II) ion by the iron(II) ion, which can change its spin state with temperature when surrounded by 2,6-bis(pyrazol-3-yl)pyridine ligands with analogous N-aryl substituents [14], would give a complex that undergoes a temperature-induced spin transition.

ACKNOWLEDGMENTS

X-ray diffraction studies were carried out using research equipment of the Center of Investigations of Molecular Structure of the Nesmeyanov Institute of Organoelement Compounds, Russian Academy of Sciences, supported by the Ministry of Science and Higher Education of the Russian Federation.

FUNDING

This study was supported by the Russian Science Foundation (grant no. 17-13-01456).

CONFLICT OF INTEREST

The authors declare that they have no conflicts of interest.

REFERENCES

1. *Spin-Crossover Materials: Properties and Applications*, Halcrow, M.A., Ed., Chichester: Wiley, 2013
2. Pavlov, A.A., Aleshin, D.Y., Nikovskiy, I.A., et al., *Eur. J. Inorg. Chem.*, 2019, vol. 2019, no. 23, p. 2819.
3. Gütlich, P., Ksenofontov, V., and Gaspar, A.B., *Coord. Chem. Rev.*, 2005, vol. 249, no. 17, p. 1811.
4. Senthil Kumar, K. and Ruben, M., *Coord. Chem. Rev.*, 2017, vol. 346, p. 176.
5. Unruh, D., Homenya, P., Kumar, M., et al., *Dalton Trans.*, 2016, vol. 45, no. 36, p. 14008.
6. Kahn, O., Kröber, J., and Jay, C., *Adv. Mater.*, 1992, vol. 4, no. 11, p. 718.
7. Ferrando-Soria, J., Vallejo, J., Castellano, M., et al., *Coord. Chem. Rev.*, 2017, vol. 339, p. 17.
8. Villalva, J., Develioglu, A., Montenegro-Pohlhammer, N., et al., *Nat. Commun.*, 2021, vol. 12, no. 1, p. 1578.
9. Halcrow, M.A., *Coord. Chem. Rev.*, 2005, vol. 249, no. 25, p. 2880.
10. Halcrow, M.A., *Coord. Chem. Rev.*, 2009, vol. 253, no. 21, p. 2493.
11. Kershaw Cook, L.J., Kulmaczewski, R., Mohammed, R., et al., *Angew. Chem., Int. Ed. Engl.*, 2016, vol. 55, no. 13, p. 4327.
12. Halcrow, M.A., *Chem. Soc. Rev.*, 2011, vol. 40, no. 7, p. 4119.
13. Halcrow, M.A., *Crystals*, 2016, vol. 6, no. 5, p. 58.

14. Nikovskiy, I., Polezhaev, A.V., Novikov, V.V., et al., *Chem.-Eur. J.*, 2020, vol. 26, p. 5629.
15. Pankratova, Y., Aleshin, D., Nikovskiy, I., et al., *Inorg. Chem.*, 2020, vol. 59, no. 11, p. 7700.
16. Nikovskiy, I.A., Polezhaev, A.V., Novikov, V.V., et al., *Crystals*, 2021, vol. 11, no. 8, p. 922.
17. Melnikova, E.K., Aleshin, D.Y., Nikovskiy, I.A., et al., *Crystals*, 2020, vol. 10, no. 9, p. 793.
18. Sheldrick, G.M., *Acta Crystallogr., Sect. A: Found. Crystallogr.*, 2008, vol. 64, p. 112.
19. Dolomanov, O.V., Bourhis, L.J., Gildea, R.J., et al., *J. Appl. Crystallogr.*, 2009, vol. 42, p. 339.
20. Evans, D.F., *J. Chem. Soc.*, 1959, p. 2003.
21. Bain, G.A. and Berry, J.F., *J. Chem. Educ.*, 2008, vol. 85, no. 4, p. 532.
22. Alvarez, S., *Chem. Rev.*, 2015, vol. 115, p. 13447.
23. Kershaw Cook, L., Mohammed, R., Sherborne, G., et al., *Coord. Chem. Rev.*, 2015, vol. 289, p. 2.
24. Alvarez, S., *J. Am. Chem. Soc.*, 2003, vol. 125, no. 22, p. 6795.
25. Pavlov, A.A., Belov, A.S., Savkina, S.A., et al., *Russ. J. Coord. Chem.*, 2018, vol. 44, no. 8, p. 489. <https://doi.org/10.1134/S1070328418080067>
26. Pavlov, A.A., Nikovskii, I.A., Polezhaev, A.V., et al., *Russ. J. Coord. Chem.*, 2019, vol. 45, no. 6, p. 402. <https://doi.org/10.1134/S1070328419060046>
27. Cavallo, G., Metrangolo, P., Milani, R., et al., *Chem. Rev.*, 2016, vol. 116, no. 4, p. 2478.
28. Craig, G.A., Costa, J.S., Roubeau, O., et al., *Chem.-Eur. J.*, 2012, vol. 18, no. 37, p. 11703.

Translated by Z. Svitanko